Journal of Oceanography, Vol. 53, pp. 467 to 480. 1997

Tidally Induced Upwelling in a Semi-Enclosed Basin: Nan Wan Bay

HUNG-JEN LEE[1], SHENN-YU CHAO[2], KUANG-LUNG FAN[1], YU-HUAI WANG[1] and NAI-KUANG LIANG[1]

[1]*Institute of Oceanography, National Taiwan University, Taipei, Taiwan, ROC*
[2]*Horn Point Environmental Laboratory, University of Maryland, Cambridge, Maryland 21613-0775, U.S.A.*

(Received 28 October 1996; in revised form 23 May 1997; accepted 23 May 1997)

Tidal flow induces sizable upwelling of cold water that intrudes onto the shallow regions of Nan Wan Bay around spring tides. The associated sudden temperature drops ranging up to 9°C or so occur in a few hours as the tide is approaching lower low water. Relaxation shortly after the sudden temperature drop is also swift but generally not as rapid as the drop. In a typical spring period, sudden temperature drops are phase locked with diurnal tides, occur daily, last several hours each, and generally diminish as the tide approaches the neap period. Moored temperature sensors in and about Nan Wan Bay near the end of 1995 allow us to approximately locate the source of cold water along the open boundary of the semi-enclosed basin. A few current meters deployed during the 1995 October~November experiment and historical point measurements of currents are also used to determine the circulation pattern associated with the cold water intrusion events. During spring tides, data suggest the development of a cyclonic recirculation eddy in the western half of the Bay near the end of lower low water. Interestingly, data do not reveal the development of an anticyclonic recirculation eddy in the flood phase of springs. Further, the recirculating cyclonic eddy seems to develop preferably around spring tides but not during normal or neap tides. The simultaneous occurrence of a cyclone and cold water intrusion suggests that the cold water at depths is funneled upward by the cyclone. Nan Wan Bay and vicinity as a year-round source of cold water appears to be maintained and modulated by the foregoing process at the fortnightly period.

Keywords:
· Sudden temperature drop,
· mooring observation,
· diurnal tides,
· tidally induced eddy.

1. Introduction

The southernmost bay of Taiwan, locally known as Nan Wan (Fig. 1), is a semi-enclosed basin bounded zonally by two capes. Distance between the two capes is about 14 km. The east cape, locally known as O-Luan-Bi (OLB), protrudes farther south than does the west cape, locally known as Mou-Bi-Tou (MBT). To the south, the Bay is open to the Luzon Strait. The semi-enclosed basin borders the Pacific Ocean to its east and Taiwan Strait to its west.

Between MBT and OLB, a zonally elongated seamount partially blocks the southward passage of the embayment to the open ocean. Maximum height of the seamount reaches about 50 m below the sea surface. There is practically no continental shelf on the west side of the embayment. On the east side, the shallow continental shelf is about 4 km wide, with isobaths running more or less in parallel with the coastline. Sandwiched between the seamount to the south and land mass to the north, the deeper portion of the embayment forms an arc-shaped channel open at both ends.

Circulation in Nan Wan Bay is dominated by strong tidal currents. The prevailing tidal currents are essentially zonal and contain sizable diurnal and semidiurnal components (Liang *et al*., 1978). Outside the embayment, tidal currents are essentially westward during flood and eastward during ebb (Li, 1987). Inside the embayment, tidal currents tend to follow isobaths over the continental shelf on the east side (Lee, 1993), but become much more complex and irregular on the west side (Liang *et al*., 1978).

From late fall to early spring, winds over Nan Wan are dominated by the northeast monsoon. The seaward wind often destratifies the water column and decreases the sea surface temperature (SST) inside the Bay. Seasonally, SST in Nan Wan is typically 22~26°C in winter but rises to 24~29°C in summer (Su *et al*., 1989). Independent of seasons, upper ocean is consistently colder inside and to the south of Nan Wan than the Pacific water to the east and South China Sea water to the west. Figure 2, derived from shipboard measurement during cruise 274 from the *R/V Ocean Researcher I*, shows the temperature field at 30 m depth on March 27, 1991. A cold anomaly in excess of 1°C

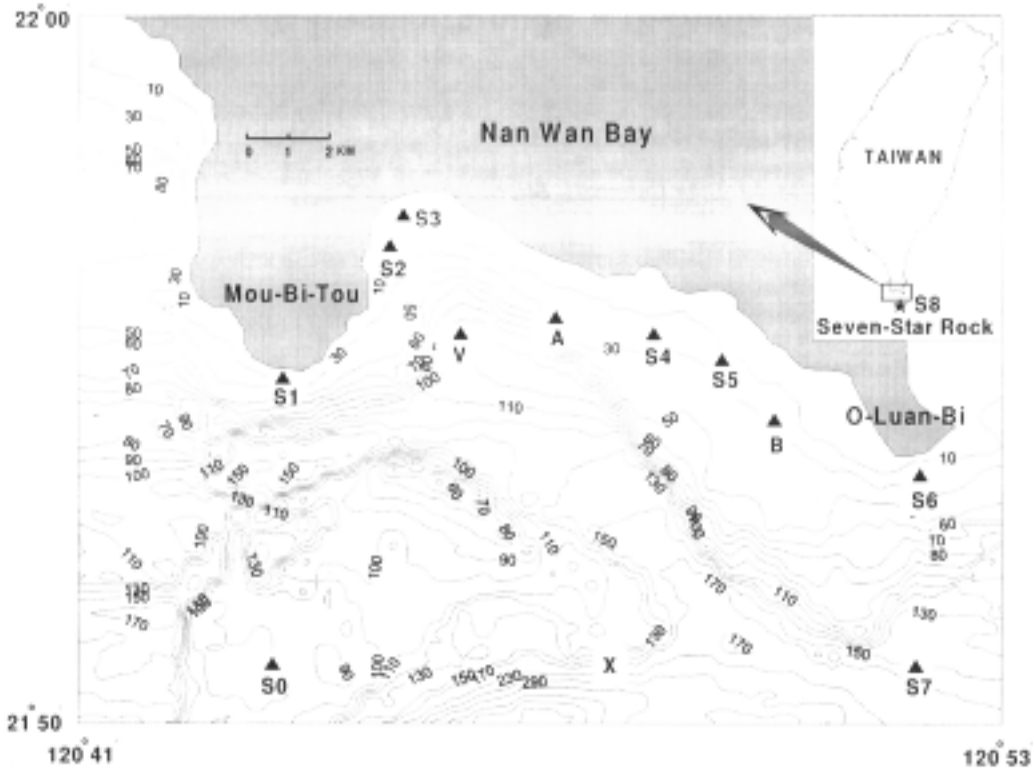

Fig. 1. Map, station locations and bottom topography of Nan Wan Bay, with depth contours in meters. Small insert at upper-right corner shows the large-scale setting and location of a remote station (Seven-Star Rock, or S8) farther south of Nan Wan Bay (see text).

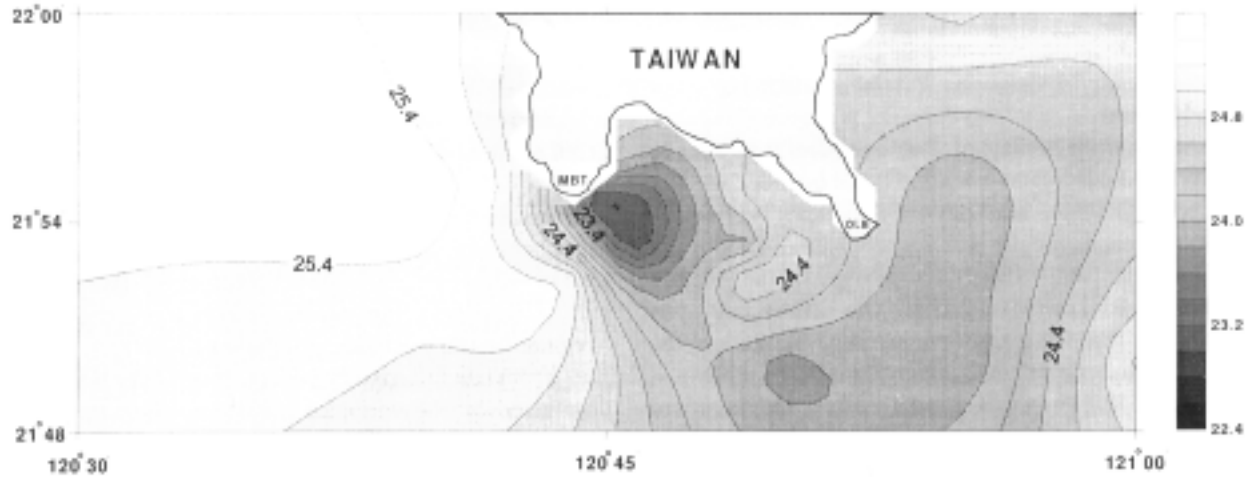

Fig. 2. Temperature field (in °C) at 30 m depth around Nan Wan Bay on March 27, 1991.

existed around Nan Wan Bay. Ship surveys in other seasons and other years show similar structure (Chen *et al*., 1994), suggesting that the synopticity problem is not the source of this cold anomaly. Clearly, the source of anomaly needs to be identified.

Observations to date have not identified any source of persistent upwelling which manifests the cold anomaly in Nan Wan and vicinity. Rather, temperature drops seem to occur intermittently and in short duration (Liang *et al*., 1978). The phenomenon was later reverified by Su *et al*. (1984).

Early interpretations of the sudden temperature drops were speculative at best. Su *et al.* (1989), for example, suggested that both the northeast monsoon and tides caused the cold anomaly. Seaward wind drives surface water offshore; the consequent upwelling could conceivably lower the water temperature. How tides affect the upwelling was not elaborated by Su *et al.* (1989). Fu (1991) further speculated that the cold water intrusion might be caused by the action of onshore currents, tides and seaward winds, and estimated that an upwelling speed of 0.13 cm/s would be necessary to cause a sudden drop of upper ocean temperature within Nan Wan Bay.

Subsequent observations using moored sensors by the first author of this paper, summarized in Lee (1995), concluded that the cold water intrusion is phase-locked with tides. In the nearshore area, the cold anomaly occurs more or less fortnightly around spring tides. The event occurs in all seasons, suggesting that the northeast monsoon in fall and winter months is not the primary force inducing the intrusion. During spring tides, Lee (1995) suggested that cold water at depths is raised by the flood current, and subsequently spilled over the shallows by the ebb current. This needs observational confirmation. The role of northeast monsoon was not elaborated in Lee (1995). Lacking spatial coverage, early interpretations were mostly speculative and did not provide a macroscopic view of how cold water intrusions occur in and around Nan Wan. Much needs to be done to elucidate the intrusion process.

Historically, spring and neap tides should be defined in terms of relative locations of the sun and moon, and are mostly related to semi-diurnal tides. Contemporary uses of the terms are much looser. The textbook definition does not work well in Nan Wan, where semidiurnal tides are often masked by diurnal tides. For want of better terms and to ease descriptions, spring and neap tides are empirically defined herein by periods of high and low tidal ranges, respectively, in a fortnightly cycle. Similar usage has been adopted by other authors, too numerous to be cited below.

The cold water intrusion events around springs induce temperature drops ranging from 3 to 10°C. Around the island of Taiwan, tidally induced, sudden temperature drops on the order of 2~3°C are quite common over canyons (Wang and Chern, 1995). The range of temperature fluctuations in Nan Wan is undoubtedly the largest and often bears socioeconomic consequences. In one drastic example on November 24, 1988, SST in the nearshore area of Nan Wan reached as low as 14°C. The sudden drop of temperature in excess of 10°C resulted in mass kill of fishes (Su *et al.*, 1989), and highlighted the importance of this phenomenon.

Systematic investigation of the cold water intrusion did not begin in earnest until the end of 1995. The observation led by a team of investigators employed 4 moored current meters (two at station V and one each at stations A and B), 5 tide gauges and 11 temperature sensors (Fig. 1). In spite of failure to retrieve instruments at station S7, the experiment is by far the most comprehensive one. Data retrieved from this experiment form the basis of this investigation. The present paper is narrowly focused on providing a first-order description of the observational results. Data interpretation follows and hopefully provides a basis for future modeling efforts.

2. Observations

Figure 3 shows the time lines of all instruments deployed near the end of 1995. Current meters were strategically deployed at station V (90 m deep) and at two stations (A and B) along 30 m isobath closer to shore. At station V, currents were recorded at intervals of 10 minutes at 45 m and 85 m depths using RCM7. Partial instrument malfunction resulted in the loss of information on current directions at 85 m depth. Stations A and B contained one RCM7 each at 15 m depth with the same sampling intervals (10 minutes).

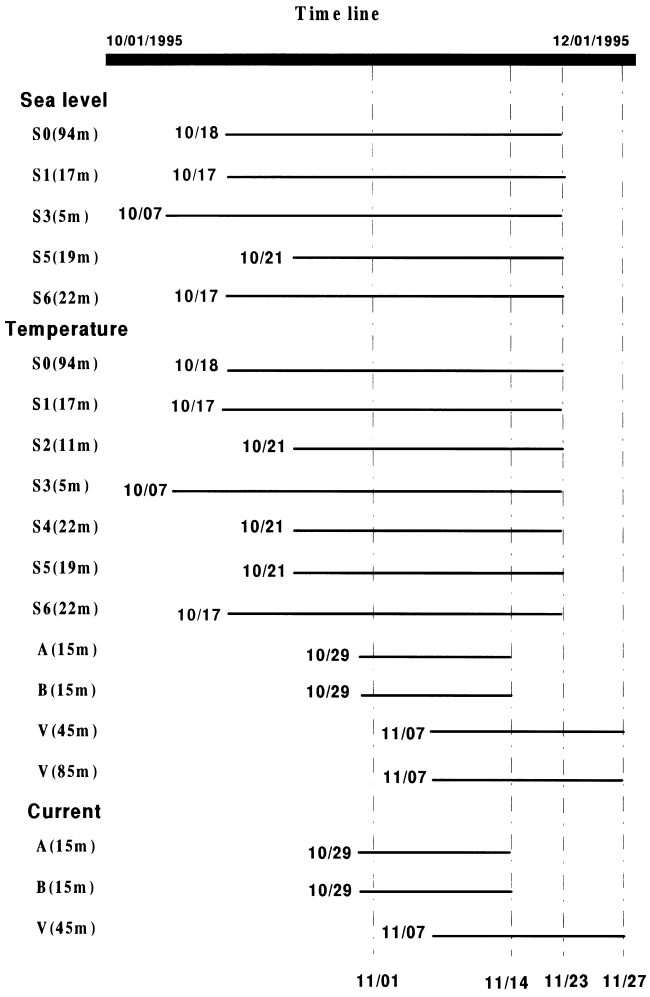

Fig. 3. Time lines of all instruments deployed near the end of 1995. Instrument depths are given after station identities.

Temperatures were also recorded with the same time intervals by the four instruments at stations V, A and B. Current fluctuations associated with sharp temperature drops elucidate the process of cold water intrusion.

Tide gauges were deployed at six stations (S0, S1, S3, S5, S6 and S7) to infer sea level fluctuations at intervals of 5 minutes. Straight lines connecting S1, S0, S7 and S6 consecutively delineate the boundaries separating Nan Wan and vicinity from adjacent seas. The tide gauge at station S7 was unfortunately lost. Driven by the modeling need to infer tidal currents within Nan Wan, a tide gauge was redeployed at station S7 in 1996 to make up the gap. Sea level information from the newly deployed tide gauge at station S7 is excluded from this report.

In addition to the four temperature time series at stations V, A and B, temperatures were also recorded at eight other stations (S0–S7) at various depths (see Fig. 3). The sampling interval at these eight stations is either 1 minute or 5 minutes. Since the cold water intrusion occurs in time scales much longer than sampling intervals, nonuniform intervals do not hinder the data analysis effort. As mentioned earlier, temperature time series at station S7 was lost due to failure to retrieve tide gauge and the temperature sensor. The remaining 11 time series of temperature listed in Fig. 3 allow us to determine the temporal and spatial variations of the cold water intrusion within Nan Wan Bay.

Beyond 1995 October~November experiment, a remote but longer time series was established sometime earlier (December, 1994~April, 1995) at Seven-Star Rock farther south of Nan Wan. The location of Seven-Star Rock, hereafter referred to as station S8, is indicated in the larger scale map in the upper-right corner of Fig. 1. At station S8, sea level fluctuations were sampled at intervals of 30 minutes while current and temperature were measured at 10 m depth every 30 minutes. Sea level fluctuations at station S8 were phase-adjusted to offset the difference in measurement period between station S8 and other stations. In essence, a time series at station S8 behaved quite differently from time series in Nan Wan and vicinity. The comparison between station S8 and any other station allows us to isolate features unique to Nan Wan.

3. Sea Level and Tidal Currents

Circulation in Nan Wan and vicinity is dominated by tidal forcing. In general, tides contain strong diurnal (Q_1, O_1, K_1) and semidiurnal (N_2, M_2, S_2) components that are

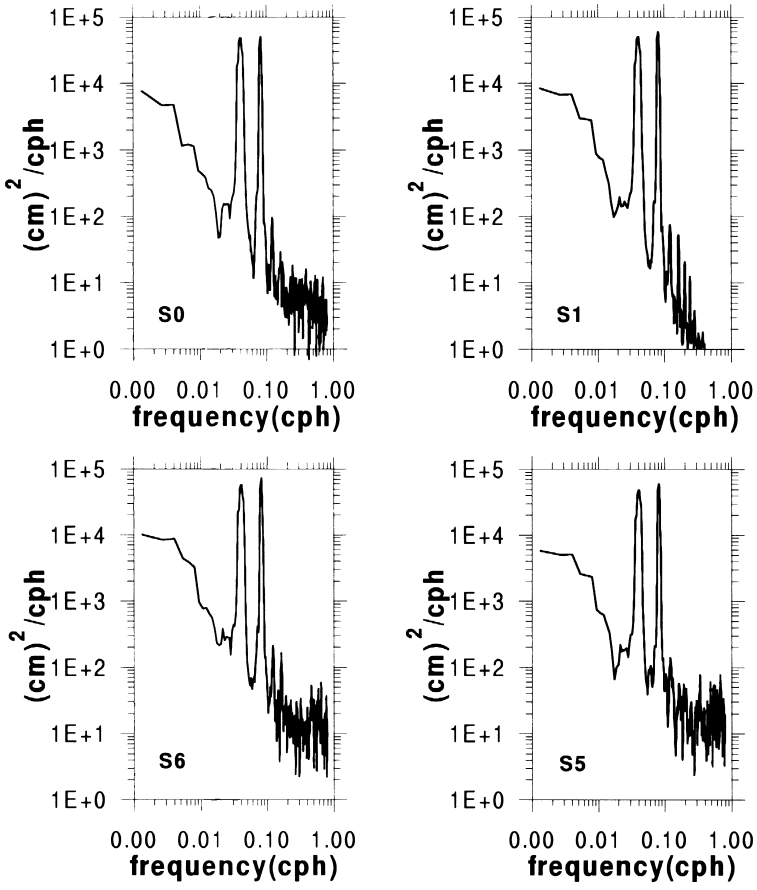

Fig. 4. Selected power spectra of sea level at stations S0, S1, S5 and S6. Frequency in unit of cph (cycles per hour).

Table 1. Amplitudes (in cm) and time lag (in hours) of dominant tidal harmonic components at four selected stations defined in Fig. 1. Time lag with reference to 11/06/09:00,1995 GMT and S8 time lag with reference to 02/09/09:00,1995 GMT.

Tides	OLB (S6)		MBT (S1)		Offshore MBT (S0)		S8	
	Amplitude	Time lag	Amplitude	Time lag	Amplitude	Time lag	Amplitude	Time lag
Q_1	5.71	15.10	3.76	17.42	3.95	15.97	3.76	14.59
O_1	21.43	15.83	20.33	16.94	19.81	16.33	18.18	15.80
K_1	22.98	15.59	22.27	16.84	21.58	16.41	19.78	17.82
N_2	5.75	6.52	4.69	7.12	4.60	6.38	5.10	6.13
M_2	28.17	6.19	24.79	7.56	23.18	6.53	30.78	6.27
S_2	12.95	6.47	11.94	7.88	10.86	6.73	14.98	7.36

modulated by a pronounced spring-neap cycle (Liang *et al*., 1978). Typical power spectra (Fig. 4) show approximately equal partition of energy between diurnal and semidiurnal components. Maximum tidal range reaches 160 cm during fortnightly spring tides. Given the complex bathymetry in the vicinity, it is reasonable to expect sizable geographic variability. Tidal range is about 160 cm at OLB and about 150 cm at MBT. Amplitudes of diurnal tides are approximately equal at MBT and OLB, while the amplitudes of semidiurnal tides at MBT are somewhat lower than those at OLB (Table 1). At station S0 offshore of MBT, tidal range decreases slightly to 150 cm. Also at MBT, diurnal tides do not decrease appreciably from MBT to S0, while semidiurnal tides decrease slightly faster in the offshore direction.

If tides propagate along the coast in form of external Kelvin waves, the characteristic speed of propagation should be about 28 m/s for an average water depth of 80 m. Given the 14 km distance between OLB and MBT, it takes about 8.3 minutes for an external Kelvin wave to travel from OLB and MBT. The observed time lag as summarized in Table 1 is much longer. Cross-spectrum analysis (Foreman and Henry, 1977) of sea level fluctuations between stations S1 and S6 suggests that OLB leads MBT by about an hour for diurnal (O_1, K_1) tides, and by more than an hour for semidiurnal (M_2, S_2) tides. Diurnal Q_1 tide and semidiurnal N_2 tide have very small amplitudes relative to other components; their phase relations do not follow the general rules stated above. Interestingly, in terms of sea level fluctuations, station S0 offshore of MBT are more or less in phase with OLB, but leads station S1 at MBT considerably. Exception exists for K_1 tide; station S0 lags OLB much more than it leads station S1. The complex phase relationship within Nan Wan dismisses a simple Kelvin wave propagation scenario. Conceivably, complicated topographies may excite Poincaré waves bouncing around the basin and distorting the phase propagation.

Moving away from Nan Wan, amplitudes of semidiurnal tides at the southernmost station (S8) at Seven-Star Rock increase considerably except for the minor N_2 component (see Table 1). In particular, the amplitudes of M_2 component far exceeds amplitudes of diurnal tides at station S8. To put tides of Nan Wan in proper perspective, it should be noted that semidiurnal tides normally dominate over diurnal tides in the coastal ocean around Taiwan (Chang, 1988). Nan Wan presents a sizable, if not unique, departure from the norm. The selective damping of semidiurnal tides within Nan Wan appears to be a highly localized phenomenon, as amplitudes of semidiurnal tides rebound to normal levels at the southern station (S8) sufficiently away from Nan Wan. Most of major diurnal and semidiurnal tidal components at station S8 lead the nearshore station of MBT (S1) except for K_1 component. The phase relations between station S8 and OLB are complex for major harmonic components. The former (S8) leads the latter (OLB) for Q_1 and N_2 tides, lags the latter for K_1, M_2 and S_2 tides, and is nearly in phase with the latter for the O_1 component.

In terms of tidal current speeds, large-amplitude topographies in Nan Wan are expected to induce sizable spatial variations. In the northern extremity of the Bay, past point measurements (Liang *et al*., 1978) suggest that tidal currents in regions shallower than 30 m are normally below 20 cm/s. Over the continental shelf along the eastern boundary of the Bay, tidal currents strengthen sharply. Specifically, flood currents during spring tides reach as high as 145 cm/s and 117 cm/s at stations A and B, respectively. Generally speaking, maximum tidal currents are the swiftest near OLB, decrease slightly near MBT, and slow down further near station A (Lee, 1993). According to Liang *et al*. (1978), tidal current speeds near MBT can be as high as 167 cm/s.

The direction of tidal currents inside Nan Wan also shows considerable spatial variation. Unpublished current data measured by the first author of this paper in the past suggest that over the continental shelf on the east side of the Bay, tidal currents regularly reverse following isobaths and correlate rather well with sea level oscillations. The previous data will not be presented below for the sake of brevity. Currents derived from the recent measurement in 1995, to be presented in Section 5, further confirms the periodic nature of tides over the continental slope on eastern side of the Bay. Tidal stream west of station A shows more complexity and

intra-tidal fluctuations. The early observation of Liang *et al*. (1978) documented reversal of nearshore tidal current on the west half of the embayment with respect to the prevailing tidal current direction to the south of the Bay, and interpreted it as part of an eddy. The size and center of the eddy, as Liang *et al*. (1978) pointed out, did not seem to be stationary. Su *et al*. (1980) employed drifter and passive tracer in Nan Wan and also confirmed the existence of the recirculation eddy. The latter study also suggested that the eddy formation occurs preferably during spring tides but not neap tides.

Summarizing, tidal currents reverse periodically along isobaths over the continental shelf on the east side of the Bay. The tidal current over the eastern shelf is northwestward during flood and southeastward during ebb. The periodic reversal does not suggest the existence of an eddy. The flow field becomes more complex west of station A, suggesting the involvement of eddy formation.

4. Cold Anomalies

Figure 5 shows a typical temperature profile in Nan Wan, measured on October 18 1995 at 21°51′ N and 120°48′ E. The location is marked by "**X**" in Fig. 1. Temperature decreases markedly with depths, leading to the cold source. Contrary to the temperature profile, salinity shows little variation with depths, maintaining a nearly constant value of 34.5 psu throughout the water column. In a highly stratified environment such as Nan Wan, upwelling of cold water must overcome considerable gravitational opposition. Sudden temperature drops in the surface water of Nan Wan often exceed 10°C and last for quite a few hours each during the ebb phase of spring tides. Tidally induced upwelling of this magnitude is quite rare, if not unique.

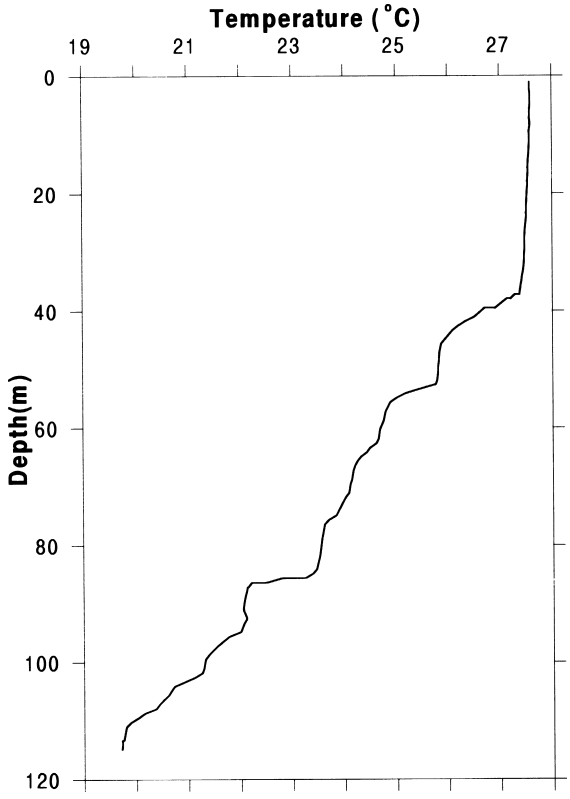

Fig. 5. A characteristic temperature profile at (21°51′ N, 120°48′ E) on October 18 1995. The station location is marked by "**X**" in Fig. 1. Salinity is nearly constant (34.5 psu) and therefore not shown.

Figure 6 shows longer time series of temperature at seven stations (from S0 to S6)from October 22 to November 22, and shorter temperature time series for station V at 45 m and 85 m depths from November 7 to 22. In this 1995 observational period, tidally induced temperature drops occurred regularly as expected. Among all stations, temperature drops at and offshore of MBT (stations S0 and S1) were either unremarkable or dissimilar to those at other stations. The frequent absence of sudden temperature drops at MBT suggests that the phenomenon is essentially confined to east of MBT. Time series of temperature at other stations were remarkably similar. Sudden temperature drops at OLB (S6) were the largest, often reaching 9°C or so. At MBT (S1), temperature drops, if any, were below noise level. Between the two capes (MBT and OLB), the northernmost station (S3) is over the shallows; temperature drops were similar to other stations but much weaker. It should also be noted that sudden temperature drops in Nan Wan do not extend farther south. At station S8, sudden temperature drops (not shown) are conspicuously absent.

Leaving the first-order similarity among stations aside, dissimilarities among stations are equally revealing and warrant discussion. We do so by dividing Nan Wan and vicinity into three regions (Fig. 7). Region I is the continental shelf area on the east side of the Bay, including stations A, B, S4, S5 and S6. Region II covers inner Bay area west of station A, including stations S2 and S3. Region III covers a portion of the arc-shaped deep channel. Since there is only one station with two temperature sensors at different depths in this region, the eastward extent of Region III is a bit uncertain.

In Region I, temperature drops were remarkably similar at all stations, peaking at station S6. In Region II, most of the sudden temperature drops in Region I were also detected. Beyond the similarity, sudden temperature drops occurred more frequently in Region II. From about October 24 to October 27, the early phase of the first spring period in Fig. 6, sudden temperature drops occurred daily in Region II, but were mostly absent in Region I, especially at station S6. The last statement is made regardless of the fact that station S3 in Region II did not exhibit much more frequent temperature drops from October 22 to October 27. Note that station S3 in the northernmost and shallowest among all stations. The phenomenon of sudden temperature drops

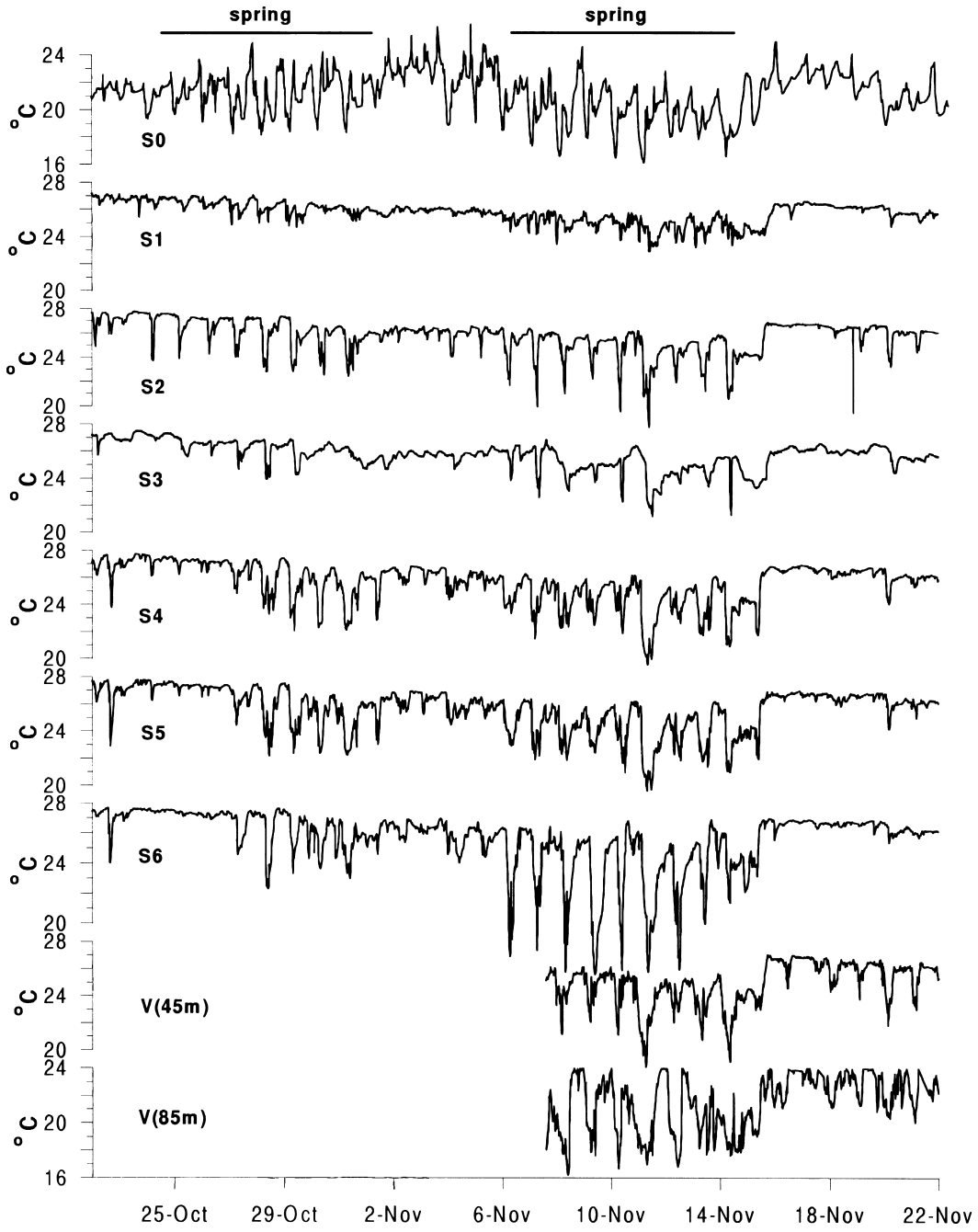

Fig. 6. Time series of temperature at seven stations (S0~S6) from October 22 to November 22 1995, covering two spring-neap cycles. Approximate time spans of two springs are shown on top. Shorter time series of temperature for station V are also shown at bottom for two different depths (45 m and 85 m).

often did not extend farther shoreward onto this shallow depth of a little over 5 m. In Region III, sudden temperature drops appeared to be bottom-trapped. These drops were largely in phase at 45 m and 85 m depths. Temperature drops at 85 m depths often exceeded 9°C, but were sometimes not followed at 45 m depths. For example, on November 12 and 13, the cold anomaly at 85 m depth was largely missed at 45 m depth. In general, temperature fluctuations at 45 m depth showed characteristic similar to those in Region I.

Sudden temperature drops are strongly modulated by spring tides (Lee, 1995). In a few days around springs, daily sudden temperature drops are the most pronounced lasting for 3–7 days. In Region I, spring tides seem to be necessary but not sufficient condition to cause sudden temperature

drops. In Region II, the probability for the occurrence of cold events is much higher than in Region I. At station V, sudden temperature drops at 85 m seem to also occur during neaps, but the intensity drops considerably. These results suggest that cold waters at depths are upwelled onto the relatively shallower Nan Wan from Region III. The intensity of upwelling appears to depend on the tidal strength. Sudden temperature drops induced by this upwelling are mostly confined in the proximity of station V during periods of weak to moderate tides, but extend farther up onto deeper reaches of Region II and, less frequently, onto Region I on the east side of the Bay during springs.

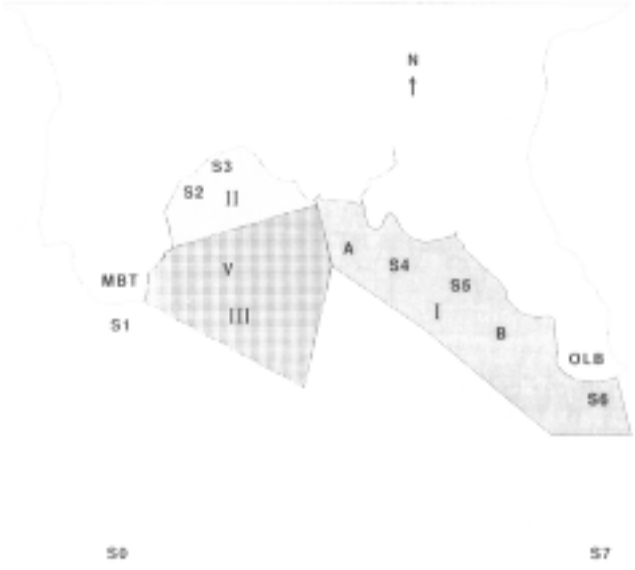

Fig. 7. Three regions where responses to cold water intrusions are different. Station locations are also shown.

Figure 8 shows time series of sea level and temperature at station S6 from November 8 to November 15. Around such a typical spring period, the two tides of the day have unequal ranges. The diurnal inequality is characterized by a higher high water followed by a lower low water, a lower high water and a higher low water. Sudden temperature drops normally begin shortly after lower low water. The temperature decreased by about 9°C in 3 hours. Subsequent temperature rises were somewhat slower. The most significant portion of the rise usually occurred between lower low water and lower high water. An entire negative pulse lasted for about 4~8 hours each. It will be emphasized later that in the central basin west of S6, sudden temperature drops occur considerably earlier, before the lower low water is reached. At a fixed station, successive temperature drops were 24 hours and 50 minutes apart, in keeping with the period of diurnal tides.

Spectral analysis of temperature time series (not shown) also reveals selective damping of semidiurnal tides in the western half of the basin (Region II). Diurnal tides dominate in all stations. However, contribution from semidiurnal

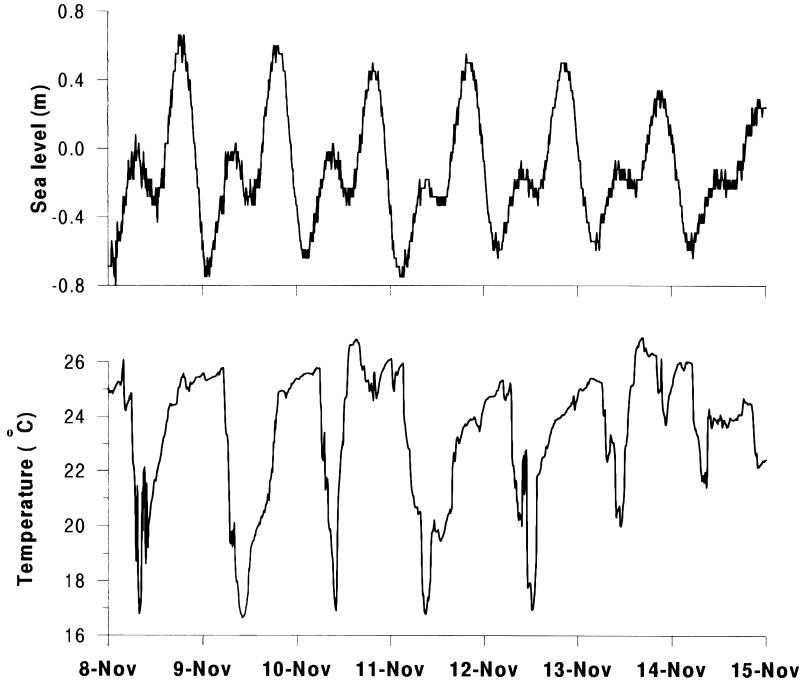

Fig. 8. Sudden temperature drops (bottom) in relation to sea level fluctuations (top) at station S6 in a seven-day (November 8~15, 1995) period around a spring tide.

Table 2. Coherence and time lag (in hours) for temperature time series between any pair of stations at the diurnal frequency. Positive time lag for X-Y means Y leads X.

Relationship	Coherence	Time lag
V (45 m)–V (85 m)	0.81	0.01
S0–V (45 m)	0.78	0.39
S1–V (45 m)	0.68	3.35
S2–V (45 m)	0.88	1.52
S3–V (45 m)	0.80	3.10
S4–V (45 m)	0.81	1.55
S5–V (45 m)	0.80	2.25
S6–V (45 m)	0.76	3.21
A–V (45 m)	0.97	0.33
S1–S0	0.76	4.47
S1–S2	0.90	1.79
S3–S2	0.86	2.20
S2–A	0.82	1.58
S3–A	0.46	3.03
S4–A	0.98	0.93
S5–A	0.98	1.72
B–A	0.89	1.95
S5–S4	0.98	0.79
S2–S4	0.80	0.73
B–S5	0.93	0.12
S6–B	0.95	0.48
S6–S5	0.81	0.57
S1–S6	0.61	0.78

Table 3. Coherence and time lag (in hours) for temperature time series between any pair of stations at the semidiurnal frequency. Positive time lag for X-Y means Y leads X.

Relationship	Coherence	Time lag
V (45 m)–V (85 m)	0.52	0.18
S0–V (45 m)	0.52	–3.42
S1–V (45 m)	0.18	4.96
S2–V (45 m)	0.44	1.16
S3–V (45 m)	0.40	0.91
S4–V (45 m)	0.46	0.14
S5–V (45 m)	0.59	1.19
S6–V (45 m)	0.43	1.83
A–V (45 m)	0.52	0.23
S1–S0	0.50	–1.46
S1–S2	0.40	–6.20
S3–S2	0.90	2.54
S2–A	0.69	2.95
S3–A	0.39	5.79
S4–A	0.88	1.71
S5–A	0.72	2.66
B–A	0.30	4.36
S5–S4	0.87	0.79
S2–S4	0.61	0.94
B–S5	0.45	1.27
S6–B	0.95	0.02
S6–S5	0.65	1.23
S1–S6	0.28	4.42

tides generally increases eastward from MBT to OLB. Similar conclusion was established in Section 3 using time series of sea level fluctuations.

Cross-spectrum of temperature time series for most pairs of stations has 10 degrees of freedom and a significance level of 0.44. Due to a shorter span of temperature time series at station V, the cross-spectrum of temperature between stations V and A has 5 degrees of freedom and a significance level of 0.78. Further, temperature coherence between stations V and B is below significance level and will not be discussed below. In the frequency domain, cross-spectra of temperature manifest a primary peak at the diurnal period and a much weaker secondary peak at semidiurnal period. Discussion below is therefore limited to the two dominant tidal frequencies.

Table 2 lists crucial statistics of the cross-spectrum analysis between stations at the diurnal frequency. Coherence between stations at the diurnal frequency is generally much above the significance level. At station V, sudden temperature drops at 45 m and 85 m depths occurred almost simultaneously. The former lags the latter only by 0.01 hour. Temperature fluctuations at station V lead all other stations. The time lag with respect to station V is the smallest at station A (0.33 hr), but largest at station S1 (3.35 hr). Coherence is generally high between stations over the continental shelf on the east side of Bay (Region I), or between stations off the continental shelf on the west side of the basin (Region II). Coherence generally decreases markedly between a station in Region I and a station in Region II. Conceivably, the poor correlation is likely a result of the continental slope, which acts as a potential vorticity barrier and reduces communications between the two regions. Conservation of potential vorticity over a steep slope greatly reduces the cross-shelf exchange of water and momentum. Although signals can travel freely along the slope, cross-shelf communications are largely prohibited.

Crucial statistics of cross-spectra at semidiurnal periods is listed in Table 3 for completeness. Coherence between stations is generally below or not much above the significance level. Occasional high coherence is mostly due to the short distance between a pair of stations.

Figure 9(a) shows schematically the phase propagation of temperature fluctuations among all stations at the diurnal frequency. That station V leads all surrounding stations indicates its proximity to the source of upwelling. Figure 9(b) further illustrates how cold water is carried onto the embayment at the diurnal frequency. Cold waters at depths are transported from around V to A preferably near the end of lower low water. Subsequent eastward spreading of cold water is faster and may be replenished by further upwelling

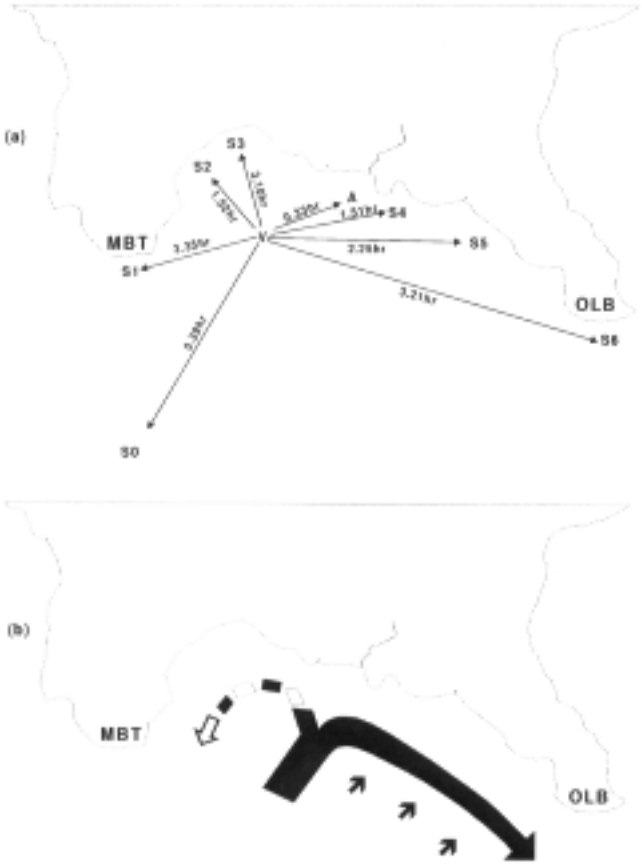

Fig. 9. (a) Inferred phase propagation of temperature fluctuations among stations at the diurnal frequency; (b) a schematic illustrating how cold waters at depths are carried onto the embayment at diurnal frequency.

from the south, as the cold anomaly intensifies from A to S6. The westward spread of cold water, on the other hand, is slower and should not be replenished by upwelling along its track westward; the cold anomaly decreases in intensity and virtually ceases to exist near station S1.

5. Flow Related to Temperature Drops

Cold water intrusion into Nan Wan usually begins near the end of lower low water, when the eastward ebb current is still strong. Temperature minimum is usually reached around lower high water (Fig. 8). During the cold water intrusion, currents at stations A, B and V and their relation to temperature fluctuations are quite complex, presenting sizable departure from simple tidal advection scenario.

Table 4 lists crucial statistics from the cross-spectrum analysis between temperature and currents at stations A, B and V. At stations A and B, coherence between temperature and currents at the diurnal frequency is below significance level and therefore not listed. The coherence is significant at the semidiurnal period, indicating some contribution of

Table 4. Coherence and time lag (in hours) between current and temperature time series at stations A, B and V. Top panel—semidiurnal frequency. Bottom panel—diurnal frequency. Zonal currents (u) are positive eastward, while meridional currents (v) are positive northward. Positive time lag for X-Y means Y leads X.

Semidiurnal		
Station A	Coherence	Time lag
u-T	0.54	2.38
T-v	0.72	4.17
Station B	Coherence	Time lag
T-u	0.46	3.57
v-T	0.52	2.62
Station V (45 m)	Coherence	Time lag
T-u	0.72	0.06
T-v	0.55	0.40
Diurnal		
Station V (45 m)	Coherence	Time lag
u-T	0.84	2.23
T-v	0.44	1.04

semidiurnal tides to the seemingly diurnal events of cold water intrusion. It is also clear from Table 4 that semidiurnal currents at A and B are not in phase. At station A, temperature (T) leads semidiurnal zonal current (u) by 2.38 hr, but lags semidiurnal meridional current (v) by 4.17 hr. The trend is reversed at station B, where T lags u by 3.57 hr but leads v by 2.62 hr.

In the arc-shaped channel, at station V, coherence is above significance level at both diurnal and semidiurnal frequencies. Whether diurnal or semidiurnal, zonal currents show much better coherence with temperature than with meridional currents. Temperature leads diurnal zonal current by about 2.23 hr, but is almost in phase with the semidiurnal zonal current. For the meridional component, both diurnal and semidiurnal currents lead temperature.

Figure 10 is a close-up of temperature and currents at stations A, B and V during one intrusion episode. The time span covers only one day (November 9, 1995). Sea level fluctuation at station S6 is also attached to the bottom of Fig. 10 to ease the comparison. Station S6 is chosen for illustration here because its temperature drops are usually the largest. Approaching the lower low water where the sudden temperature drop occurs, flow at station V turned from northeastward to southwestward rather quickly. Concurrently, flow at station A changed from southeastward to northwestward, while flow at station B remained southeastward throughout. The sudden turning was completed in about two hours. Temperatures at stations A and V dropped markedly in the process; the former was more pronounced. Further at station V, the temperature drop is much more

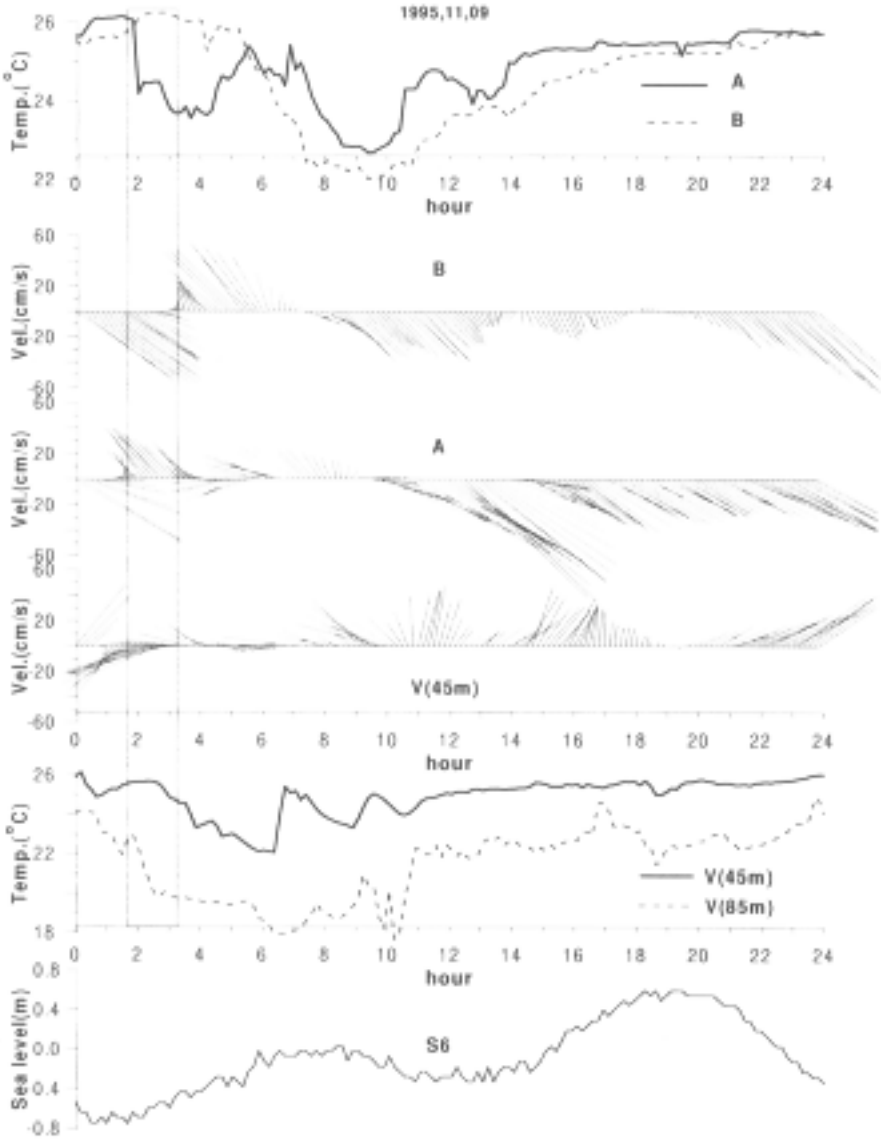

Fig. 10. A close-up of current vectors in relation to temperature and sea level fluctuations in one day (November 9, 1995). Currents are shown at stations A and B, and at 45 m depth at station V, with north directed toward the top of the diagram. Temperatures are shown at stations A and B (top panel), and at 45 m and 85 m depths at station V (5th panel). Tidal elevation at station S6 is shown in the bottom panel. Two vertical bars cutting through the top five panels mark the period of cold water intrusion and sudden flow changes in the western and central portions of the Bay (stations A and V).

pronounced at 85 m depth than at 45 m depth. Thereafter, currents at stations A and V maintained a strong westward component with minor meridional oscillations at intra-tidal frequencies. The intra-tidal meridional oscillations in a primarily westward flow lasted for about 8 hours at station V. Thereafter, normal current oscillations at tidal frequencies resumed and temperature began to rise at station V. For both temperature and currents, the cold water intrusion of tidal origin entailed intra-tidal oscillations especially in the central and western portions of the semi-enclosed basin (see currents at stations A and V in Fig. 10).

It would be helpful to construct a few tidal ellipses to illustrate variability of tidal currents in Nan Wan. The following difficulties prevented us from doing so. Currents are available at only three stations (A, B and V); three ellipses are hardly representative of the geographic variability. Among the three stations, two (A and V) exhibit intra-tidal oscillations; tidal ellipses therefore cannot be cleanly defined at the two stations. Currents at station B are essentially alongshore; the tidal ellipse looks like a straight

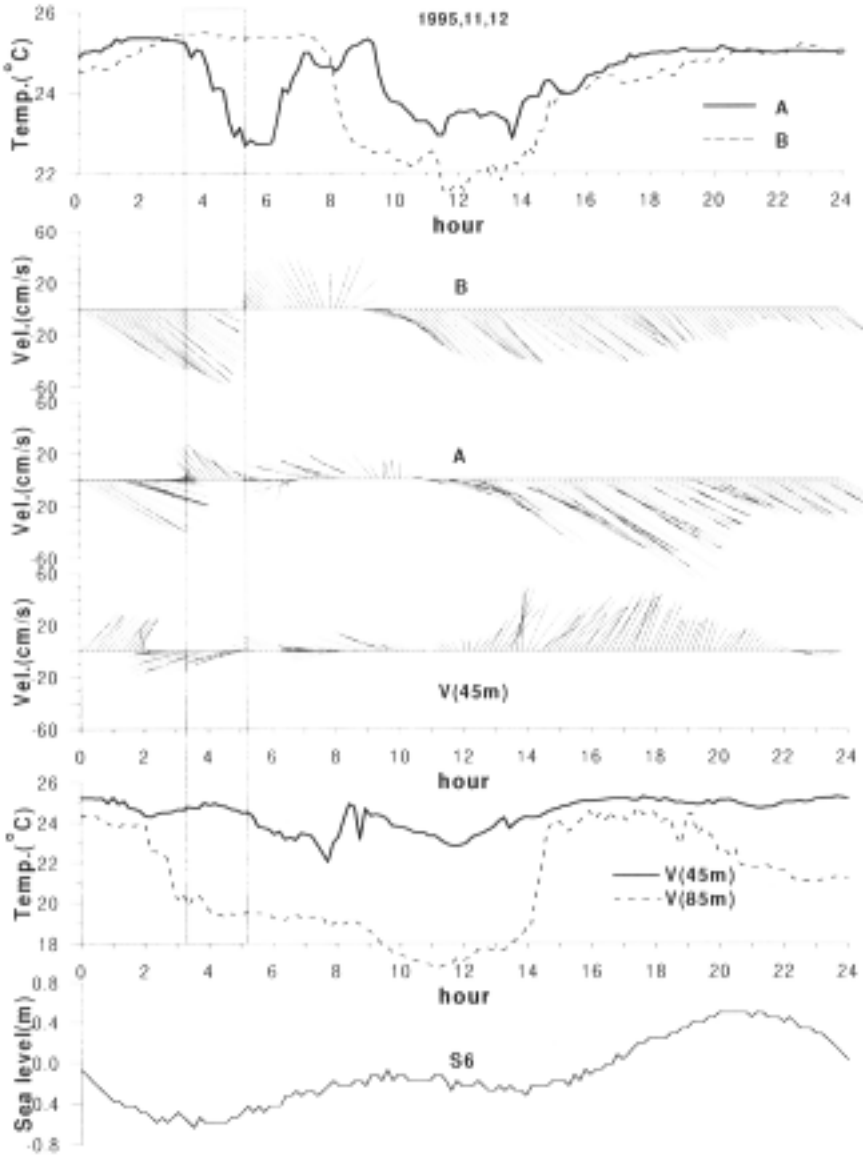

Fig. 11. A close-up of current vectors in relation to temperature and sea level fluctuations in one day (November 12, 1995). Currents are shown at stations A and B, and at 45 m depth at station V, with north directed toward the top of the diagram. Temperatures are shown at stations A and B (top panel), and at 45 m and 85 m depths at station V (5th panel). Tidal elevation at station S6 is shown in the bottom panel. Two vertical bars cutting through the top five panels mark the period of cold water intrusion and sudden flow changes in the western and central portions of the Bay (stations A and V).

line segment rather than an ellipse and is therefore not shown.

It should also be noted that the intrusion event as shown in Fig. 10 essentially repeats itself almost daily during the spring period. It is difficult to illustrate this point from week-long or month-long time series. To emphasize the repetitive nature of the cold water intrusion, Fig. 11 shows another close-up of the event on November 12 1995. The similarities between Figs. 10 and 11 are striking.

6. Discussion and Conclusions

Prior to this work, point measurements in both space and time around Nan Wan breed speculations about how cold water intrusions occurred. Some speculations, such as tidal generation, stand the test of time; some, such as wind modulation, remain speculative. Further, past observations were inadequate in spatial coverage to provide a macroscopic view of how cold waters intrude into Nan Wan. The recent observational network at the end of 1995 is the most com-

prehensive to date, allowing us to better define the mesoscale origin of the cold water intrusion process in this region.

The interplay between the onset of sudden temperature drops and tidal currents around springs is intriguing inside Nan Wan. Approaching the lower low water, currents at station V suddenly shift from northeastward to southwestward. Shortly thereafter, current at station A shifts from southeastward to northwestward. These intra-tidal fluctuations are not detected at station B. Temperature at station A begins to drop at this time. Currents at station V continue to be unsteady for a few more hours; high-frequency meridional fluctuations accompany the primarily westward flow. Temperature at station V will not rise until the end of the unsteadiness. During the onset of sudden temperature drops, diverging tidal current between stations A and B lasts for about two hours (Fig. 10). Flow continuity requires a northward flow from deep waters to the south to maintain the divergence. Not surprisingly, temperature records indicate this is the onset of massive upwelling of cold water from depths.

Figure 10 suggests the existence of a recirculation eddy in the central and western portions of the basin as the tide is approaching lower low water around springs. The southeastward current at station B (Fig. 10) can be viewed as shoreward extension of prevailing tidal current from deeper waters to the south, manifesting an anticyclonic meander crest in the eastern half of the basin (Region I). It is also clear that the cyclonic eddy is confined to east of MBT, for otherwise the cold event would be detectable at station S1. During the cold intrusion, the primarily westward current at station V is about 30 cm/s on the average and persists for about 8 hours. This suggests a westward expansion distance of 8.64 km for cold anomalies if the current remains zonally uniform for some distance. The 8.64 km distance is much greater than the distance between stations S1 and V. The lack of cold episode at station S1 is therefore a strong evidence that the recirculation cyclonic eddy is confined to east of MBT. The existence of a recirculation eddy associated with ebb current during springs had been suggested earlier (Liang *et al*., 1978; Su *et al*., 1980) based on point measurements of currents and fisherman description. The 1995 experiment lends support to the existence of the recirculating cyclone, and better defines its horizontal extent and timing.

Figure 12 conceptualizes the circulation pattern during and shortly after the onset of cold water intrusion. This is a composite picture. While the circulation inside Nan Wan is derived from the present observation, the prevailing tidal current south of the Bay is inferred from tidal models of Li (1987) and Lee (1993).Conceivably, the developing cyclone would induce upwelling through either bottom Ekman suction or centrifugal acceleration and should be responsible for part of the cold anomaly. As for the centrifugal acceleration, a close analogy can be drawn from meteorology; the low pressure center associated with a tornado sucks ground materials aloft. To better quantify the dynamical balance of the recirculation eddy, let the eddy radius (r) be 2 km and the characteristic swirling speed (v_0) be 50 cm/s (see Fig. 10, station A). Taking a Coriolis parameter (f) of about 5×10^{-5} s^{-1}, the centrifugal acceleration (v_0^2/r) is about 1.25×10^{-2} cm/s^2, while the Coriolis acceleration (fv_0) is about 2.5×10^{-3} cm/s^2. Thus during the initial phase of cold water intrusion, the developing cyclonic eddy seems to be more cyclostrophic than geostrophic. The estimate is necessarily crude; better estimates require much refined observational network. We do not know whether relaxation of sudden temperature drops requires downwelling. Conceivably, relaxation could occur without downwelling. As the cyclonic eddy and the associated anticyclonic meander (Fig. 12) dissipate, upwelling should cease. Subsequent tidal stream could sweep the cold anomaly out of the Bay and cause the temperature to rise again, setting the stage for the next intrusion event.

Fig. 12. A schematic showing the development of a cyclonic recirculation eddy near the end of ebb phase in springs. Open arrow indicates ascending shoreward flow feeding the diverging flow between stations A and B.

Although the recirculation cyclone seems to develop near the end of ebb current, nearshore temperature reaches minimum in the beginning phase of flood. Apparently, the cyclonic eddy, once developed, is able to self-perpetuate for some time even after the turning of tides. Further, the anticyclonic meander crest to the east of the cyclone (Fig. 12) carries deeper offshore water to the shallow embayment and may also decrease the temperature. In this context, readers should be reminded that Fig. 12 illustrates the flow but not the pathway of cold water intrusion. Given the circulation pattern, cold water should first appear near the

center of cyclonic eddy, which is likely close to station V, and to the east of the eddy caused by the advection of anticyclonic meander. Multiple sources of cold water suggest that the subsequent spreading is much more complex than one would like to derive from Fig. 12 following a simple advection scenario. Whether the cyclonic eddy or the anticyclonic meander crest is chiefly responsible for the cold water intrusion is a question clearly beyond the scope of this investigation. A numerical model is very much in need to unravel it.

During springs, the present experiment supports the existence of a cyclonic eddy during the ebb current, but oddly enough, fails to identify anticyclonic eddies during the flood current at least in the western half of the basin. The flood-ebb asymmetry in the development of recirculation eddies is of dynamical interest and should eventually be resolved using a numerical model. Leaving this dynamical question aside, the dominance of cyclonic eddies during ebb over anticyclonic eddies during floods lends further support to our interpretation that the cyclonic eddy and cold water intrusion are strongly inter-related. Not surprisingly, Nan Wan proves to be a year-round source of cold surface water (Chen *et al.*, 1994).

One reviewer raised an interesting but different possibility that the cold water intrusion might be a manifestation of internal tide generation around Nan Wan. The idea is not new. Wang and Chern (1995), for example, attributed the occurrence of cold anomalies over a canyon to the generation of internal tides. The alternative mechanism and our interpretation are not mutually exclusive. It may be that the cold anomalies are somehow generated by internal tides, and subsequently carried into the Bay by the recirculation eddy and meandering tidal stream. However, if one follows the internal tide scenario exclusively, then there is a suite of questions waiting to be answered. For example, why are internal tides preferably excited during the ebb period? How do internal tides induce recirculation eddies inside the Bay? The present observational network is inadequate to either support or dismiss the internal tide scenario. Much more intensive efforts are needed to confirm it. In closing, we leave the possibility of cold anomalies as manifested by internal surges open for debate, and emphasize that it may coexist with the mechanism envisaged in this work.

Acknowledgements

Authors HJL and KLF were supported by the National Science Council of the Republic of China under grant NSC 85-2611-M-002A-010; YHW appreciated the logistical support from Dr. W. S. Chuang in the field experiments. SYC was supported by U.S. National Science Foundation under grant OCE95-04959. Mr. Ting-Yu Kuo, Pei-Jie Meng, Chao-Chang Lin and Tai-Hsien Yang provided invaluable assistance during the field phase of this work. Comments from two reviewers and Associate Editor, Shoshiro Minobe, greatly improve the presentation of this paper.

References

Chang, I.-J. (1988): Calculation of high tides along the west coast of Taiwan. Master Thesis, Inst. of Oceanography, National Taiwan Ocean Univ., 47 pp. (in Chinese).

Chen, C. T. A., S.-C. Ou, Y.-C. Chung, C.-K. Wu and L.-R. Chun (1994): Research of living resources around the nuclear power plant in southern Taiwan. Tech. Rep. 20, College of Marine Sciences, National Sun Yat-Sen Univ., 195 pp. (in Chinese).

Foreman, M. G. G. and R. F. Henry (1977): Tidal Analysis Based on High and Low Water Observations. Institute of Ocean Sciences, Patricia Bay, Sidney, British Columbia, Pacific Marine Science Report, No. 77-10, 101 pp.

Fu, S.-B. (1991): Tidal and wind modulations of water temperature in Nan Wan. Master Thesis, Inst. of Oceanography, National Taiwan Univ., 53 pp. (in Chinese).

Lee C.-K. (1995): Effects of tides and winds on water temperature in Nan Wan. Master Thesis, Inst. of Oceanography, National Taiwan Univ., 60 pp. (in Chinese).

Lee, H.-J. (1993): Tidal numerical model and residual currents in Nan Wan Bay. Master Thesis, Inst. of Oceanography, National Taiwan Univ., 69 pp. (in Chinese).

Li, H.-W. (1987): A numerical predicative model of tides in the seas adjacent to Taiwan. *Proceedings of National Science Council, Part A: Physical Science and Engineering*, Vol. 11, No. 1, 74–89.

Liang, N. K., S. L. Lien, W. C. Chen and H. T. Chang (1978): Oceanographic investigation in the vicinity of Ma-An-San and Nan Wan Bay. Special publication No. 18, Inst. of Oceanography, National Taiwan Univ., 207 pp.

Su, J.-C., T.-C. Hung, Y.-M. Chiang, T.-H. Tan, K.-H. Chang, K.-T. Shao, P.-P. Hwang, K.-T. Lee, C.-C. Huang, C.-Y. Huang, K.-L. Fan and S.-Y. Yeh (1980): An ecological survey on the waters adjacent to the nuclear power plant in southern Taiwan. Special publication No. 7, National Scientific Committee on Problems of the Environment, Academia Sinica, Taipei, Taiwan, ROC, 115 pp. (in Chinese).

Su, J.-C., T.-C. Hung, Y.-M. Chiang, T.-H. Tan, K.-H. Chang, K.-T. Shao, P.-P. Hwang, K.-T. Lee, C.-C. Huang, C.-Y. Huang, K.-L. Fan and S.-Y. Yeh (1984): An ecological survey on the waters adjacent to the nuclear power plant in southern Taiwan. Special publication No. 27, National Scientific Committee on Problems of the Environment, Academia Sinica, Taipei, Taiwan, ROC, 214 pp. (in Chinese).

Su, J.-C., T.-C. Hung, Y.-M. Chiang, T.-H. Tan, K.-H. Chang, K.-T. Shao, P.-P. Hwang, K.-T. Lee, C.-C. Huang, C.-Y. Huang, K.-L. Fan and S.-Y. Yeh (1989): An ecological survey on the waters adjacent to the nuclear power plant in southern Taiwan. Special publication No. 70, National Scientific Committee on Problems of the Environment, Academia Sinica, Taipei, Taiwan, ROC, 238 pp. (in Chinese).

Wang, J. and C.-S. Chern (1995): Preliminary Observation of Internal Surges in Tung-Kang. *ACTA Oceanography Taiwanica*, **35**, 17–40.